



ELSEVIER

Available online at [www.sciencedirect.com](http://www.sciencedirect.com)

SCIENCE @ DIRECT®

Earth and Planetary Science Letters 214 (2003) 369–378

EPSL

[www.elsevier.com/locate/epsl](http://www.elsevier.com/locate/epsl)

# Lattice distortion in ice crystals from the Vostok core (Antarctica) revealed by hard X-ray diffraction; implication in the deformation of ice at low stresses

Maurine Montagnat<sup>a,\*</sup>, Paul Duval<sup>a,\*\*</sup>, Pierre Bastie<sup>b</sup>, Bernard Hamelin<sup>c</sup>,  
Volodya Ya. Lipenkov<sup>d</sup>

<sup>a</sup> *Laboratoire de Glaciologie et Géophysique de l'Environnement, CNRS, BP 96, 38402 St. Martin d'Hères Cedex, France*

<sup>b</sup> *Laboratoire de Spectrométrie Physique, CNRS, BP 87, 38402 St. Martin d'Hères Cedex, France*

<sup>c</sup> *Institut Laue Langevin, BP 156X, 38042 Grenoble Cedex 9, France*

<sup>d</sup> *Arctic and Antarctic Research Institute, St. Petersburg 199397, Russia*

Received 15 January 2003; received in revised form 18 June 2003; accepted 25 June 2003

## Abstract

Hard X-ray diffraction experiments have been carried out on ice monocrystals taken from the 3623 m long Vostok core (Antarctica). Strain gradients associated with the storage of geometrically necessary dislocations appear to be a general feature of the deformation microstructure of ice. The observed lattice distortion is related to the bending of the basal plane and the torsion of the lattice around the *c*-axis. The lattice distortion is shown to be compatible with the basal dislocations generally observed in ice crystals, supporting the assumption of deformation modes governed by basal slip and accommodated by recrystallization processes. The dependence of the ice viscosity on grain size in ice sheets appears to be compatible with these accommodation modes.

© 2003 Elsevier B.V. All rights reserved.

*Keywords:* ice; ice sheets; creep; deformation inhomogeneities; X-ray diffraction

## 1. Introduction

Understanding how polar ice sheets interact with the climatic system is of the highest impor-

tance to predict sea-level changes and to assess the effect of massive discharge of icebergs on the ocean circulation [1]. The dating of deep ice cores requires ice-sheet flow modeling [2]. The development of physically based models describing ice-sheet dynamics has recently received special attention [3]. Knowledge of the rheological properties of ice at low stresses is of great importance when modeling ice-sheet flow [4]. A flow relationship with a stress exponent *n* lower than 2 at deviatoric stresses lower than 0.1 MPa is now widely accepted [5–10]. Although there is no broad agree-

\* Corresponding author. Tel.: +33-4-76-82-42-67/  
+33-4-76-82-42-18; Fax: +33-4-76-82-42-01.

\*\* Corresponding author. Tel.: +33-4-76-82-42-67/  
+33-4-76-82-42-18; Fax: +33-4-76-82-42-01.

E-mail addresses: [maurine@lgge.obs.ujf-grenoble.fr](mailto:maurine@lgge.obs.ujf-grenoble.fr)  
(M. Montagnat), [duval@lgge.obs.ujf-grenoble.fr](mailto:duval@lgge.obs.ujf-grenoble.fr) (P. Duval).

ment as to the rate-controlling processes, intracrystalline basal slip is generally the dominant deformation process for this region of low  $n$  values [7,10]. Note that basal slip is assumed to be the dominant deformation mechanism in most deformation models used to simulate the development of fabrics (distribution of the orientation of the  $c$ -axes) in ice sheets [11–14]. Goldsby and Kohlstedt [15,16] question this assumption and propose superplastic flow with grain boundary sliding as the dominant deformation mode for the flow regime in ice sheets. However, fabric development and the microstructures observed in ice sheets are not compatible with this superplastic flow mechanism [17].

This paper presents results of hard X-ray diffraction experiments used to observe the lattice distortion of several ice crystals collected along the 3623 m Vostok ice core (East Antarctica). This deep ice core has provided a record of past climate and atmospheric composition over the last four glacial–interglacial cycles [2]. Below 3538 m, the ice core consists of lake ice developed above subglacial lake Vostok [18]. This ice is characterized by exceptionally large crystals with a very high crystalline quality [19]. Samples were especially selected from interglacial climatic stages as this ice is characterized by relatively large grain size [20]. One lake ice sample was also studied for comparison.

The observed lattice curvature supports basal slip as the predominant deformation mode in ice sheets. Results are analyzed in the context of the deformation of plastically non-homogeneous materials [21,22].

Due to the large viscoplastic anisotropy of the ice crystal, grains that are well oriented for basal slip (soft grains) deform much more than hard grains. Stress equilibrium and strain compatibility are maintained at the expense of the build-up of deformation inhomogeneities within grains [23]. The bending of basal planes and kink bands were observed in experimentally deformed specimens [23,24]. As shown by Nye [21] and Ashby [22], dislocations, called *geometrically necessary dislocations* (GNDs), are stored to accommodate these strain gradients. Dislocations piled up at grain boundaries or edge dislocations accommo-

dating the bending of basal planes can be considered as GNDs. In polycrystals, the density of GNDs scales with the gradient of plastic strain, which increases with decreasing grain size [22]. Like all dislocations stored within grains, GNDs contribute to strain hardening and can therefore be at the origin of the increase of hardening when grain size is decreasing. In ice sheets, grain growth and dynamic recrystallization should partially relieve internal stresses associated with such strain gradients [25]. The density of dislocations would increase by strain hardening and decrease by the formation and the migration of grain boundaries. At the opposite of the hardening by GNDs, the efficiency of recovery processes described above is the highest in fine-grained ices [25]. Cuffey et al. [26,27] have recently presented convincing arguments for an *increase* in strain rate with *decreasing* grain size in ice sheets. The relationship between the density of dislocations associated with strain gradients, strain hardening and grain size [28] cannot therefore be extrapolated for polar ice.

Special emphasis is placed here on the analysis of mechanisms involved in the deformation of ice sheets and compatible with a grain size-dependent rheology. The aim of this study is to show that dislocation creep is compatible with in situ deformation measurements and with most of the data on the microstructure of ice in ice sheets.

## 2. Dislocations and the deformation of single crystals of ice

The main feature of the plasticity of ice crystals is its outstanding anisotropy. Ice essentially deforms by the glide of dislocations on the basal plane. The resistance to shear on non-basal planes is large and can be 60 times higher than resistance on the basal planes [29]. Basal slip is caused by the glide motion of basal dislocations with the  $\langle 11\bar{2}0 \rangle$  Burgers vector. The rapid glide of short edge dislocations on  $\langle 1\bar{1}00 \rangle$  prismatic planes was observed by X-ray topography [30,31]. The fact that basal slip is dominant, in spite of faster movement of dislocations on non-basal planes, is attributed by these authors to the large difference in the length of dislocations. On the other hand,

the dissociation of basal dislocations into partial dislocations impedes the glide of these dislocations on prismatic planes [32].

Non-homogeneous deformation of single crystals was observed by Nakaya [33] by performing bending tests. Strain gradients associated with the bending of basal planes were accommodated by homogeneously distributed basal edge dislocations (GNDs). The formation of tilt sub-boundaries was also observed at high strain. Concerning the lattice distortion associated with basal screw dislocations, original results were obtained by X-ray diffraction technique on ice single crystals deformed in torsion [34]. The torsion strain appears to be totally accommodated by geometrically necessary basal screw dislocations. Dislocations are also stored in ice single crystals homogeneously deformed in tension and compression [35]. The dislocations that trap each other randomly are referred to as *statistically stored dislocations* [22]. In ice polycrystals, the large mismatch of slip at the boundaries induces large deformation inhomogeneities. The density of GNDs should be higher than the density of statistically stored dislocations [34].

### 3. The X-ray diffraction technique

The X-ray diffraction experiments were carried out at the Institut Laue Langevin (ILL) in Grenoble, using an industrial high-voltage X-ray tube (420 kV) and the original Laue hard X-ray technique that allows the in situ observation of bulk samples more than 1 cm thick [36]. This technique is based on a focusing effect which occurs when a divergent X-ray beam diffracts through a crystal. (Fig. 1a). It can be noted on a 3D representation (Fig. 1b) that the diffraction spots have the shape of lines. The width of the diffraction lines is directly related to the lattice distortion [36], while the position along the lines corresponds to the diffraction of a virtual slice of the crystal perpendicular to the line. This allows one to separate the contribution of the diffracting lines when the crystal is inhomogeneous. The presence of subgrains will be revealed by the splitting of the lines.

The energy range for the white divergent beam

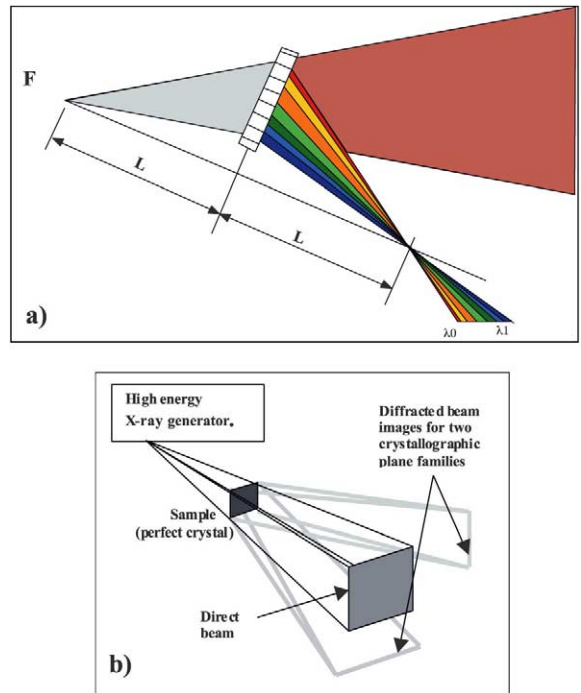


Fig. 1. (a) Schematic diagram of focusing property. (b) 3D diffraction view for a perfect single crystal.

is between 100 and 400 keV, giving wavelengths between 0.03 and 0.12 Å. Bragg angles being low, the diffraction peaks are located close to the direct beam. This allows the simultaneous observation of peaks from several crystallographic planes on the detector which is composed of an X-ray intensifier and a CCD camera for fast acquisition of diffraction patterns. Angular lattice distortion from 10 sec of arc (10'') up to a few degrees, depending on the sample–beam source distance, can be determined with this technique. The setup used for the present study has a measurement accuracy of better than 1 min of arc (1'), taking into account the other broadening effects (size of the filament of the X-ray tube and thickness of the sample).

Fig. 2a,b gives a diffraction pattern schematically represented, similar to what is obtained with ice. The orientation of the sample compared to the direct beam direction is given, together with the lattice distortion measurements. The lattice distortion can be due to randomly located dislo-

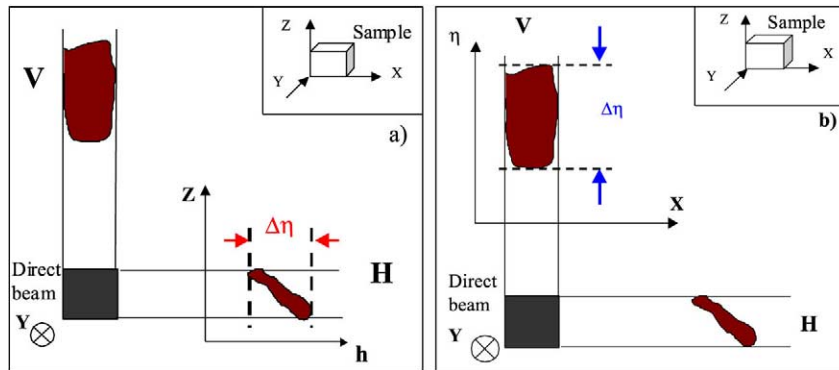


Fig. 2. Diffraction patterns as can be observed for ice. (a) Horizontal diffraction; the  $\eta$ -axis corresponds to the angular lattice misorientation around the  $Z$ -axis.  $\Delta\eta$  represents a continuous lattice distortion from the top to the bottom of the sample. (b) Vertical diffraction; the  $\eta$ -axis corresponds to the angular lattice misorientation around the  $X$ -axis.  $\Delta\eta$  represents a combination of mosaicity and spatial lattice distortion from the left to the right of the sample.

cations, creating a homogeneous enlargement of the diffraction line called mosaicity; this distortion is uniform throughout the sample. Dislocations can also be arranged continuously within the crystal, creating lattice distortions (such as bending) that are represented by a continuous inclination of the lines ( $\Delta\theta$ ) from one side of the sample to the other. Both diffraction line characteristics (mosaicity and inclination) can be analyzed in terms of dislocation density. However, in the case of mosaicity, no simple direct relationship can be established due to the random spatial distribution of dislocations [37].

#### 4. Diffraction patterns of Vostok ice crystals

Several samples from the deepest part of the 3623 m Vostok ice core were studied. Information on samples is given in Table 1. The temperatures at which the samples were deformed in the in situ conditions are between  $-10$  and  $-5^\circ\text{C}$ . The illuminated area of the samples was first chosen close to the sample size for a general examination. Then vertical and horizontal slits were used to determine the spatial arrangement of dislocations.

The diffraction pattern of a sample extracted from a large monocrystal of the Vostok subglacial lake ice at 3610 m depth is shown in Fig. 3. This ice was refrozen from the subglacial lake water [38] and is supposed to be different from the gla-

cier ice which constitutes the main part of the core (until 3539 m). The width of the diffraction peaks and their inclination approach the accuracy limit of the set-up used. A slight continuous lattice distortion ( $\Delta\theta \approx 1'$ ) over the sample can, however, be observed on both basal and prismatic diffraction lines. Such a low lattice distortion is similar to the one observed on very carefully grown artificial ice single crystals [19]. These results support the assumption concerning ice flow near the lake and indicate very low strain rates in lake ice [19]. The observation of such very low-distortion crystals

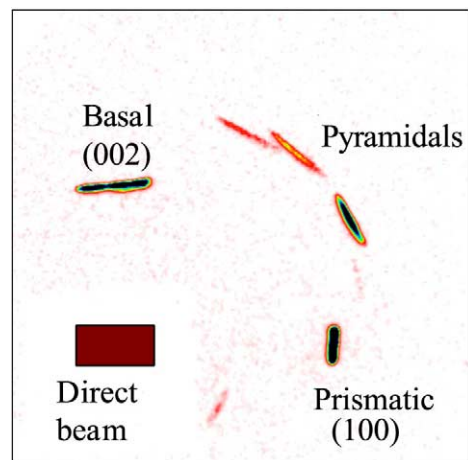


Fig. 3. Diffraction patterns for the Lake Vostok ice sample V3610. Several crystallographic orientations are observed: the basal (002), prismatic (100) and several pyramidal planes.

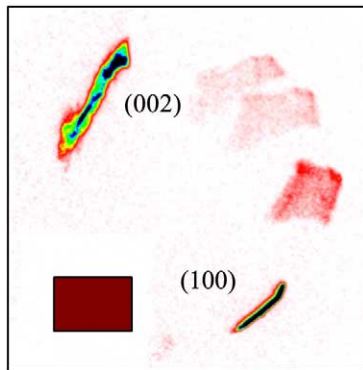


Fig. 4. Diffraction patterns for the glacier ice sample V3516. Several crystallographic orientations are observed: the basal (002), prismatic (100) and several pyramidal planes.

shows that the process of coring and the storage of samples at  $-20^{\circ}\text{C}$  do not induce additional lattice distortion.

Figs. 4–6 show the diffraction patterns of three glacier ice samples from 3516, 3493 and 2755 m in depth. A significant observation is the strong difference in the distortion observed on the prismatic and basal planes. Let us first consider the prismatic planes. The very low variation of the width of the diffraction lines with the volume studied is related to low mosaicity on the prismatic planes. This width appears to be similar to that of undeformed samples and approaches the accuracy limit of the equipment (between  $1'$  and  $2'$  for samples V3516 and V3493 and slightly higher for sample V2755). On the other hand, the strong and irregular inclination of the lines shows a continuous distortion of the lattice from the bottom to the top of the sample, i.e. along the  $Z$ -axis (which is also the  $c$ -axis). This distortion corresponds to a torsion of the lattice around the  $c$ -axis induced by screw dislocations homogeneously located on the basal plane. Values of distortion of about  $10'$  per

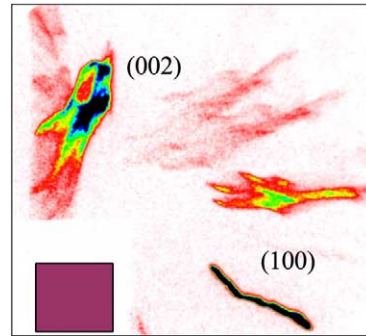


Fig. 5. Diffraction patterns for the glacier ice sample V3493. Several crystallographic orientations are observed: the basal (002), prismatic (100) and several pyramidal planes.

centimeter of sample illuminated, in height, are observed on the three samples (note that the change in distortion direction is not relevant, as the orientation of the sample in the core is not known).

The shape of the reflections on the basal planes is different. An inclination of the basal diffraction line is clearly visible on samples V3516 and V3493, indicating a continuous distortion of the lattice in the  $X$ - $Z$  plane, around the  $X$ -axis (Figs. 4 and 5). This continuous inclination is, respectively,  $18'$  and  $37'$  per centimeter of sample illuminated, in width. However, the main difference concerns the mosaicity, which seems much higher than that observed on the prismatic lines. The diffraction pattern for sample V2755 is more complicated (Fig. 6). Contrary to the previous samples, systematic analysis by rotation around the  $X$ -axis reveals several peaks, indicating the presence of subgrains with misorientations of between  $10'$  and  $18'$ . This effect was analyzed more systematically with an horizontal slit of 1 mm in order to check at the same time the size and location of the subgrains (Fig. 6b).

Table 1  
Characteristics of samples studied. For dimension orientation see Fig. 2

| Sample (depth)           | Orientation of the $c$ -axis | $X \times Z \times Y$ dimensions     |
|--------------------------|------------------------------|--------------------------------------|
| Vostok (3610 m): 'V3610' | vertical                     | $14 \times 9 \times 7 \text{ mm}^3$  |
| Vostok (3516 m): 'V3516' | vertical                     | $16 \times 11 \times 3 \text{ mm}^3$ |
| Vostok (3493 m): 'V3493' | vertical                     | $19 \times 19 \times 8 \text{ mm}^3$ |
| Vostok (2755 m): 'V2755' | vertical                     | $\approx 1.5 \text{ cm}^3$           |

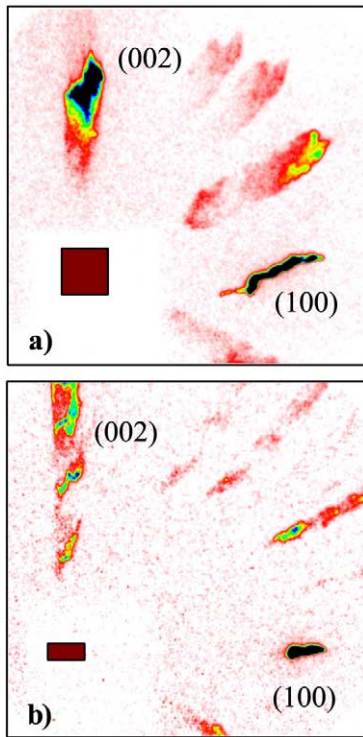


Fig. 6. Diffraction patterns for the glacier ice sample V2755. Several crystallographic orientations are observed: the basal (002), prismatic (100) and several pyramidal planes. (a) Overview of the whole sample. Subgrains are observable on the basal and pyramidal diffraction lines. (b) Observation of subgrains was made possible by the rotation around the  $X$ -axis with the use of a horizontal slit of 1 mm.

Due to the effect of sample thickness, it is difficult to separate the continuous inclination from the mosaicity. Fig. 7 represents the diffraction pattern of sample V3493 associated with cross-sections giving the diffracting volume distribution along the line. While the enlargement of the basal diffraction line of sample V3493 could have been fully associated with mosaicity at first sight, two peaks appear on the vertical cross-section. Both peaks have a low width at half-height, similarly to the thin peak of the horizontal cross-section, associated with the prismatic diffraction line. This observation assesses the presence of two subgrains continuously distorted with little mosaicity but superimposed on each other. Similar characteristics are observed on cross-sections done all over the diffraction lines, although only one is reported

in the figure. This thus shows the predominance of the continuous inclination on the basal diffraction line compared to mosaicity.

The continuous inclination of the basal diffraction lines is fully compatible with a continuous bending of the basal planes accommodated by the distribution of basal edge dislocations.

To summarize, the lattice distortion of the studied glacier samples appears to be related to the bending of basal planes and the torsion of the lattice around the  $c$ -axis. Subgrains with a misorientation of basal planes lower than  $1^\circ$  are observed for sample V2755. The mosaicity of basal diffraction peaks seems to be higher than that of prismatic diffraction peaks.

### 5. Analysis of lattice distortion in terms of the spatial distribution of dislocations

The observed lattice distortions can be analyzed in terms of the nature, arrangement and density

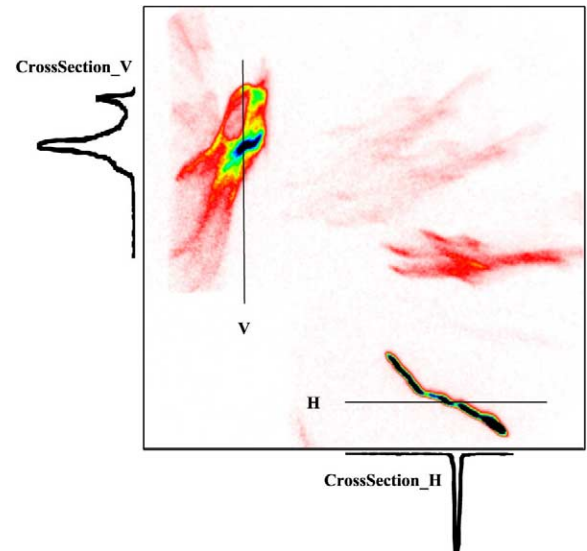


Fig. 7. Diffraction pattern for sample V3493 associated with horizontal and vertical cross-sections giving the diffracting volume distribution along the prismatic and the basal diffraction lines, respectively. The horizontal cross-section indicates a low mosaicity and a continuous lattice distortion. The vertical cross-section indicates a combination of mosaicity and spatial lattice distortion; the presence of two peaks is associated with subgrains of low mosaicity.

of dislocations. These distortions are compatible with the nature of the dislocations observed in ice [39,40].

The torsion of the lattice around the  $c$ -axis can be perfectly described by the arrangement of basal screw dislocations. Similarly, as shown by several authors [21,24], the bending of basal planes is explained by the arrangement of edge basal dislocations. Boundaries of subgrains observed on the basal diffraction peaks (Fig. 6) can also be composed of basal edge dislocations [41].

The analysis shows a relatively large lattice inclination of diffraction lines compared to mosaicity. Most of the dislocations are then expected to be geometrically necessary as defined by Ashby [22]. The corresponding density can be calculated from the following relation:

$$\rho_{\text{geom}} = \frac{\theta}{bL} \quad (1)$$

where  $\theta$  is the distortion angle over the length  $L$  of the sample illuminated by the X-ray beam.  $L$  is the  $X$ -dimension when considering inclination of the basal line, and the  $Z$ -dimension for the prismatic case.  $b$  is the Burgers vector [21].

Table 2 gives the density of GNDs deduced from the measured lattice distortion in samples V3493 and V3516. Assuming that the density of dislocations associated with mosaicity is negligible, the calculated density of screw dislocations of about  $10^9 \text{ m}^{-2}$  is close to that of edge dislocations. This dislocation density can be compared with that deduced for interglacial ice along the Vostok core by de La Chapelle et al. [20]. The calculated dislocation density from a simple phys-

ical deformation model increases from the surface down to about 1000 m depth, where it reaches a value of about  $1.3 \times 10^{11} \text{ m}^{-2}$ . The dislocation density rapidly decreases below 1000 m to reach a value of about  $10^{10} \text{ m}^{-2}$  at 3316 m, where the calculation was stopped. A dislocation density lower than  $10^{10} \text{ m}^{-2}$  is therefore expected at the depths of 3493 and 3516 m. The high temperature in the deepest parts of the core and the small horizontal shear stress are the reason for the relatively low calculated dislocation density near the bottom of the core. The density of GNDs deduced from X-ray diffraction measurements, however, must be considered as a lower bound since dislocations associated with mosaicity and the pile-ups of dislocations at grain boundaries were not taken into account. As indicated by X-ray diffraction experiments, the contribution of the mosaicity to the total dislocation density should be low in Vostok ice samples. As regards the pile-ups of dislocations, it is important to emphasize that grain boundary migration associated with grain growth and recrystallization impedes their formation by absorbing dislocations located in the volume swept by the mobile grain boundaries [20]. It is also important to point out that this study was limited to ice samples corresponding to the interglacial climatic stages, for which the grain boundary migration rate and grain size are significantly higher than in glacial ice. The pinning of grain boundaries by micro-particles, whose number is very high in glacial ice, explains this difference [42]. As a consequence, a dislocation density higher than estimated in this study should be found in glacial ice.

Table 2

Angular lattice distortions related to the continuous inclination of the diffraction peaks, and calculated density of geometrically necessary dislocations

| Sample | Diffraction peak | $\theta$ angular distortion ('/cm) | $\rho_{\text{geom}}$ ( $\text{m}^{-2}$ ) |
|--------|------------------|------------------------------------|--|
| V3516  | prismatic        | 10                                 | $6 \times 10^8$                          |
|        | basal            | 18                                 | $10^9$                                   |
| V3493  | prismatic        | 13                                 | $8 \times 10^8$                          |
|        | basal            | 37                                 | $2 \times 10^9$                          |

Angles are measured in min of arc per centimeter of sample illuminated by the direct beam ( $X$ -dimension for basal diffraction peak,  $Z$ -dimension for prismatic one).

## 6. Discussion

### 6.1. Role of strain gradients in the deformation of ice at low stresses

The hard X-ray diffraction experiments provide precise information on the distribution of dislocations in the studied Vostok ice samples. The bending of basal planes and the torsion of the lattice around the *c*-axis by GNDs appear to be a general feature of the ice microstructure during the deformation. The observed tilt sub-boundaries of low misorientation (Fig. 6) could be associated with the formation of new grain boundaries by the progressive misorientation of subgrains in orientation gradients. This nucleation mechanism associated with the low-velocity grain boundary migration regime occurs extensively along the Vostok ice core [20]. This recrystallization regime is referred to as rotation recrystallization by the geological community [43].

Strain gradients are induced by the mismatch of slip at the boundaries [28]. The required GNDs contribute to strain hardening and render the deformation between grains compatible [22]. The large difference in strain rate between monocrystals oriented for basal slip and polycrystals is related to the build-up of a non-uniform internal stress field [44]. The associated hardening is governed by GNDs accommodating the distortion of the lattice. It is significant to note that the lattice distortion associated with the pile-up of dislocations at grain boundaries could not be observed as only monocrystals were analyzed. This long-range hardening is kinematic (or directional) and associated with the large recovery creep observed after unloading [45]. As discussed above, low-stress conditions in ice sheets and grain boundary migration should impede the formation of pile-ups of dislocations in ice sheets.

In an isotropic ice polycrystal, stress equilibrium and strain compatibility can be assured by introducing only basal slip and prismatic (or pyramidal) slip [46,47]. Note that the bending of basal planes could contribute to the deformation along the *c*-axis. It may represent an additional ice crystal deformation mode in the same way as pyramidal slip in polycrystal models.

### 6.2. Rate-controlling processes

We assume that the deformation of polar ice at low stresses is produced by intracrystalline slip, which is accommodated by the formation and migration of grain boundaries associated with recrystallization. Strain gradients contribute to the stress equilibrium and deformation compatibility between grains [48]. The hardening associated with the GNDs associated with these strain gradients is related to grain size: smaller grains are stiffer than large grains [22,49]. But, as mentioned above, recovery processes which occur in ice sheets should overcome this grain-size effect induced by strain gradients.

The deformation model based on the equilibrium between strain hardening and recovery by Montagnat and Duval [25] can be used as a starting point to analyze a grain-size effect induced by recrystallization processes. The dislocation density is used as an internal variable.

The change in dislocation density  $d\rho$  during deformation is given by:

$$\frac{d\rho}{dt} = \frac{\dot{\epsilon}}{bD} - \frac{\theta_c K}{bD^3} - \frac{\alpha \rho K}{D^2} \quad (2)$$

where  $\dot{\epsilon}$  is the strain rate,  $b$  is the Burgers vector,  $D$  the grain size,  $\theta_c$  the misorientation angle when a low-angle boundary becomes a high-angle boundary,  $K$  the grain boundary migration rate and  $\alpha$  a coefficient higher than one that accounts for the higher dislocation density near grain boundaries.

The first term in Eq. 2 is related to the Orowan equation [50]. The other terms correspond respectively to the dislocations required for the formation of grain boundaries (new grain nucleation) and the dislocations absorbed by grain boundary migration. A constant grain size is observed in several ice cores when grain growth is balanced by grain nucleation. The steady-state strain rate, if obtained, depends on both dislocation density and grain size. Only qualitative arguments can be advanced since there is an interrelation between grain size, dislocation density and strain rate, both grain size and  $\rho$  depending on stress. From Poirier [43], recrystallized grain size is inversely proportional to stress with a power exponent equal to 1.2. Considering the grain-size depen-

dence of the two recovery mechanisms (Eq. 2), the ice viscosity at low stress should decrease with decreasing grain size. This agrees with the analysis of field data given by Cuffey et al. [26,27].

## 7. Conclusion

X-ray diffraction experiments performed on glacier ice have provided new information on the microstructure of ice after deformation. Mechanisms for ice deformation at low stresses have been specified on the basis of the results obtained for the lattice distortion of ice crystals from the Vostok ice core. Indeed, we suggested that the observed bending of basal planes is accommodating basal slip, allowing the deformation along the  $c$ -axis. Strain gradients appear to characterize the deformation of ice polycrystals. They contribute to strain hardening, stress equilibrium and deformation compatibility. Orientation gradients require the presence of GNDs and appear to be the first stage of grain nucleation. Basal slip associated with the bending of basal planes and grain growth or recrystallization are the dominant deformation modes for polar ice.

The grain-size dependence of the ice viscosity deduced from field data [26] appears to be compatible with the deformation modes suggested.

## Acknowledgements

We are very thankful to O. Brissaud for the design of the cooling device and the help during the experiments, as well as to G. Quemard. We thank ILL staff and particularly C. Menthonnex and A. Elaazzouzi for technical and computing assistance. This research was supported by CNRS (SPI and SDU departments). We acknowledge J.R. Petit for his interest and all Russian participants in drilling at Vostok. **[BARD]**

## References

- [1] C.J. Van der Veen, Fundamentals of Glacier Dynamics. A.A. Balkema, Rotterdam, 1999, 462 pp.
- [2] J.R. Petit and 18 co-authors, Climate and atmospheric history of the past 420,000 years from the Vostok ice core, Antarctica, *Nature* 399 (1999) 429–436.
- [3] A.J. Payne and 10 co-authors, Results from the EIS-MINT model intercomparison: the effects of thermomechanical coupling, *J. Glaciol.* 46 (2000) 227–238.
- [4] W.F. Budd, T.H. Jacka, A review of ice rheology for ice sheet modelling, *Cold Reg. Sci. Technol.* 16 (1989) 107–144.
- [5] M. Mellor, R. Testa, Creep of ice under low stress, *J. Glaciol.* 8 (1969) 147–152.
- [6] D. Dahl-Jensen, N.S. Gunderstrup, Constitutive properties of ice at Dye 3, Greenland, in: *Physical Basis of Ice Sheet Modelling*, vol. 170, AIHS, Vancouver, 1987, pp. 31–43.
- [7] R.B. Alley, Flow law hypothesis for ice sheet modeling, *J. Glaciol.* 38 (1992) 441–446.
- [8] P. Duval, O. Castelnaud, Dynamic recrystallization of ice in polar ice sheets, *J. Phys. C* 3 (1995) 197–205.
- [9] V.Y. Lipenkov, A. Salamatin, P. Duval, Bubbly-ice densification in ice sheets: applications, *J. Glaciol.* 43 (1997) 397–407.
- [10] P. Pimienta, P. Duval, Rate controlling processes in the creep of polar glacier ice, *J. Phys. C* 1 (1987) 243–248.
- [11] N. Azuma, A. Hashi, Formation processes of ice fabric patterns in ice sheets, *Ann. Glaciol.* 6 (1985) 130–134.
- [12] R.B. Alley, Fabrics in polar ice sheets: development and prediction, *Science* 240 (1988) 493–495.
- [13] O. Castelnaud, P. Duval, R.A. Lebensohn, G.R. Canova, Viscoplastic modeling of texture development in polycrystalline ice with a self-consistent approach: comparison with bound estimates, *J. Geophys. Res. B* 6 (1996) 13851–13868.
- [14] Th. Thorsteinsson, Fabric development with nearest-neighbor interaction and dynamic recrystallization, *J. Geophys. Res.* 107 B (2002) ECV3 1–13.
- [15] D.L. Goldsby, D.L. Kohlstedt, Grain boundary sliding in fine-grained ice I, *Scr. Mater.* 37 (1997) 1399–1406.
- [16] D.L. Goldsby, D.L. Kohlstedt, Superplastic deformation of ice: experimental observations, *J. Geophys. Res. B* 106 (2001) 11017–11030.
- [17] P. Duval, M. Montagnat, Comments on ‘Superplastic deformation of ice: experimental observations’ by D.L. Goldsby and D.L. Kohlstedt, *J. Geophys. Res.* 107 B (2002) ECV4 1–2.
- [18] J. Jouzel, J.R. Petit, R. Souchez, N. Barkov, V.Ya. Lipenkov, D. Raynaud, M. Stievenard, N.I. Vassiliev, V. Verbeke, F. Vimeux, More than 200 meters of lake ice above subglacial lake Vostok, Antarctica, *Antarct. Sci.* 286 (1999) 2138–2141.
- [19] M. Montagnat, P. Duval, P. Bastie, B. Hamelin, O. Brissaud, M. de Angelis, J.R. Petit, V.Ya. Lipenkov, High crystalline quality of large single crystals of subglacial ice above Lake Vostok (Antarctica) revealed by hard X-ray diffraction, *C. R. Acad.* 333 (2001) 419–425.
- [20] S. de La Chapelle, O. Castelnaud, V.Ya. Lipenkov, P. Duval, Dynamic recrystallization and texture develop-

- ment in ice as revealed by the study of deep ice cores in Antarctica and Greenland, *J. Geophys. Res. B* 103 (1998) 5091–5105.
- [21] J.F. Nye, Some geometrical relations in dislocated crystals, *Acta Metall.* 1 (1953) 153–162.
- [22] M.F. Ashby, The deformation of plastically non-homogeneous materials, *Philos. Mag.* 13 (1970) 399–424.
- [23] C.J.L. Wilson, Y. Zhang, Comparison between experiment and computer modelling of plane-strain simple-shear ice deformation, *J. Glaciol.* 40 (1994) 46–55.
- [24] P. Mansuy, A. Philip, J. Meyssonier, Localization of deformation in polycrystalline ice, *J. Phys. IV France* 11 (2001) 267–274.
- [25] M. Montagnat, P. Duval, Rate controlling processes in the creep of polar ice, influence of grain boundary migration associated with recrystallization, *Earth Planet. Sci. Lett.* 183 (2000) 179–186.
- [26] K.M. Cuffey, T. Thorsteinsson, E.D. Waddington, A renewed argument for crystal size control of ice sheet strain rates, *J. Geophys. Res. B* 105 (2000) 27889–27894.
- [27] K.M. Cuffey, H. Conway, A. Gades, B. Hallet, C.F. Raymond, S. Whitlow, Deformation properties of subfreezing glacier ice: role of crystal size, chemical impurities, and rock particles inferred from in-situ measurements, *J. Geophys. Res. B* 105 (2000) 27895–27915.
- [28] N.A. Fleck, G.M. Muller, M.F. Ashby, J.W. Hutchinson, Strain gradient plasticity: theory and experiments, *Acta Metall. Mater.* 42 (1994) 475–487.
- [29] P. Duval, M.F. Ashby, I. Anderman, Rate controlling processes in the creep of polycrystalline ice, *J. Phys. Chem.* 87 (1983) 4066–4074.
- [30] A. Higashi, A. Fukuda, T. Hondoh, K. Goto, S. Amakai, Dynamical dislocation processes in ice crystal, in: T. Suzuki, K. Ninomiya, S. Takeuchi (Eds.), *Proceedings of Yamada Conference IX*, University of Tokyo Press, Tokyo, 1985, pp. 511–515.
- [31] S. Ahmad, R.W. Whitworth, Dislocation motion in ice: a study by X-ray synchrotron topography, *Philos. Mag. A* 57 (1988) 749–766.
- [32] T. Hondoh, H. Iwamatsu, S. Mae, Dislocation mobility for nonbasal glide in ice measured by in situ X-ray topography, *Philos. Mag. A* 62 (1990) 89–102.
- [33] U. Nakaya, Mechanical properties of single crystals of ice, U.S. Army Snow Ice and Permafrost Research Establishment Research Report 28 (1958) 1–46.
- [34] M. Montagnat, P. Duval, P. Bastie, B. Hamelin, Strain gradient and geometrically necessary dislocations in deformed ice single crystals, *Scripta Mat.* 49 (2003) 411–415.
- [35] Y. Okada, T. Hondoh, S. Mae, Basal glide of dislocations in ice observed by synchrotron radiation topography, *Philos. Mag.* 79 (1999) 2853–2868.
- [36] B. Hamelin, P. Bastie, A new hard X-ray diffractometer (100–400 keV) for bulk crystalline analysis. Applications for non-destructive investigation, *Proc. SPIE* 4786 (2002) 29–39.
- [37] A. Borbély, H. Driver, T. Hungar, An X-ray method for the determination of stored energies in texture components of deformed metals: application to cold worked ultra high purity iron, *Acta Mater.* 48 (2000) 2005–2016.
- [38] R. Souchez, J.R. Petit, J.L. Tison, J. Jouzel, V. Verbeke, Ice formation in subglacial Lake Vostok, Central Antarctica, *Earth Planet. Sci. Lett.* 181 (2000) 529–538.
- [39] S.J. Jones, N.K. Gibra, X-ray topographical study of dislocations in pure and HF-doped ice, *Philos. Mag.* 27 (1973) 457–472.
- [40] A. Fukuda, A. Higashi, X-ray diffraction topographic studies of dislocations in natural large ice single crystals, Japan, *J. Appl. Phys.* 8 (1969) 993–999.
- [41] A. Fukuda, H. Shoji, Dislocations in natural ice crystals, in: *Lattice Defects in Ice Crystals*, Hokkaido University Press, Sapporo, 1988, pp. 13–25.
- [42] J. Weiss, J. Vidot, M. Gay, L. Arnaud, P. Duval, J.R. Petit, Dome Concordia microstructure: impurities effect on grain growth, *Ann. Glaciol.* 35 (2002) 552–558.
- [43] J.P. Poirier, *Creep of Crystals*, Cambridge University Press, New York, 1985.
- [44] M.F. Ashby, P. Duval, The creep of polycrystalline ice, *Cold Reg. Sci. Technol.* 11 (1985) 285–300.
- [45] P. Duval, Anelastic behaviour of polycrystalline ice, *J. Glaciol.* 21 (1978) 621–628.
- [46] J.W. Hutchinson, Creep and plasticity of hexagonal polycrystals as related to single crystal slip, *Metall. Trans.* 8A (1977) 1465–1469.
- [47] O. Castelnaud, G.R. Canova, R.A. Lebensohn, P. Duval, Modelling viscoplastic behavior of anisotropic polycrystalline ice with a self-consistent approach, *Acta Mat.* 45 (1997) 4823–4834.
- [48] S. Sun, B.L. Adams, W.E. King, Observations of lattice curvature near the interface of a deformed aluminium bicrystal, *Philos. Mag.* 80 (2000) 9–25.
- [49] V.P. Smyshlyaev, N.A. Fleck, The role of strain gradients in the grain size effect for polycrystals, *J. Mech. Phys. Solids* 44 (1996) 465–495.
- [50] E. Orowan, Problems of plastic gliding, *Proc. Phys. Soc.* 52 (1940) 8–22.